

# A negative feedback between anthropogenic ozone pollution and enhanced ocean emissions of iodine

C. Prados-Roman<sup>1</sup>, C. A. Cuevas<sup>1</sup>, R. P. Fernandez<sup>1,\*</sup>, D. E. Kinnison<sup>2</sup>, J-F. Lamarque<sup>2</sup> and A. Saiz-Lopez<sup>1</sup>

[1]{Atmospheric Chemistry and Climate Group, Institute of Physical Chemistry Rocasolano (CSIC), Madrid, Spain}

[2]{Atmospheric Division, NCAR, Boulder, CO, USA}

[\*]{now at: National Scientific and Technical Research Council (CONICET), UTN-FR Mendoza/ICB-UNCuyo, Mendoza, Argentina}

Correspondence to: A. Saiz-Lopez (a.saiz@csic.es)

## Abstract

Naturally emitted from the oceans, iodine compounds efficiently destroy atmospheric ozone and reduce its positive radiative forcing effects in the troposphere. Emissions of inorganic iodine have been experimentally shown to depend on the deposition to the oceans of tropospheric ozone, whose concentrations have significantly increased since 1850 as a result of human activities. A chemistry-climate model is used herein to quantify the current ocean emissions of inorganic iodine and assess the impact that the anthropogenic increase of tropospheric ozone has had on the natural cycle of iodine in the marine environment since pre-industrial times. Our results indicate that the human-driven enhancement of tropospheric ozone has doubled the oceanic inorganic iodine emissions following the reaction of ozone with iodide at the sea surface. The consequent build-up of atmospheric iodine, with maximum enhancements of up to 70% with respect to preindustrial times in continental pollution outflow regions, has in turn accelerated the ozone chemical loss over the oceans with strong spatial patterns. We suggest that this ocean-atmosphere interaction represents a negative

1 geochemical feedback loop by which current ocean emissions of iodine act as a natural buffer  
2 for ozone pollution and its radiative forcing in the global marine environment.

3

## 4 **1 Introduction**

5 Tropospheric ozone ( $O_3$ ) is a short-lived greenhouse gas (GHG) with a positive radiative  
6 forcing (RF) of  $0.4 \text{ W m}^{-2}$  ( $0.2\text{-}0.6 \text{ W m}^{-2}$ ) (Myhre et al., 2013). The main precursors of this  
7 GHG are  $NO_x$  ( $NO$  and  $NO_2$ ), hydrocarbons,  $CO$ ,  $CH_4$  and stratospheric downward transport;  
8 whereas its main sinks include photodissociation, deposition and reactions with the chemical  
9 families of odd oxygen, hydrogen, nitrogen and halogens (Brasseur and Solomon 2005; Myhre  
10 et al., 2013).

11 About a decade ago iodine oxide was detected in the marine boundary layer (MBL) (Alicke et  
12 al., 1999). Since then, several studies have aimed at determining the source gases of iodine  
13 and their chemical pathways (see Saiz-Lopez et al., 2012a and references therein). While  
14 emissions of very-short lived (VSL) organic source gases ( $CH_3I$ ,  $CH_2I_2$ ,  $CH_2ICl$  and  $CH_2IBr$ )  
15 have been observed in supersaturated waters (Carpenter et al., 2012), the existence of an  
16 abiotic ocean source of iodine has been directly and indirectly inferred throughout scattered  
17 field campaigns and 1-D model works (Read et al., 2008; Jones et al., 2010; Mahajan et al.,  
18 2010 and 2012; Gómez Martín et al., 2103; Grossman et al., 2103; Lawler et al., 2014). Very  
19 recently, laboratory studies have demonstrated the potential of the ocean to emit inorganic  
20 hypoiodous acid (HOI) and, to a lesser extent molecular iodine ( $I_2$ ), following the reaction of  
21 ozone with iodide at the sea surface (Carpenter et al., 2013; MacDonald et al., 2014). The  
22 oceanic emission of inorganic iodine source gases (ISG; i.e., HOI,  $I_2$ ) has been experimentally  
23 shown to depend on the deposition of tropospheric ozone to the oceans, wind speed and sea  
24 surface temperature (SST) (Garland et al., 1980; Carpenter et al., 2013; MacDonald et al.,  
25 2014).

26 Given that anthropogenic activities have led to an increase of 20-55% in tropospheric ozone  
27 since 1850 (Myhre et al., 2013) and that the current halogen-mediated tropospheric ozone  
28 loss in the tropical regions accounts for  $-0.1 \text{ W m}^{-2}$  of the radiative flux at the tropical  
29 tropopause (i.e.,  $\sim 1/3$  of the total tropospheric  $O_3$  RF, Saiz-Lopez et al., 2012b), this study  
30 aims at (i) assessing how the anthropogenic increase in tropospheric ozone have affected the  
31 abiotic oceanic emission of ISG, and (ii) describing a geochemical feedback mechanism  
32 between ozone and iodine that mitigates the positive radiative forcing of tropospheric ozone

1 in the global marine environment. In this work Sect. 2 provides details on the setup of the  
2 chemistry-climate model employed in this study, while the results for pairs of model runs for  
3 different periods of time are discussed in Sect. 3. The summary and conclusions are presented  
4 in Sect. 4.

5

## 6 **2 Methods**

7 The chemical simulations in this study were performed with the 3-D CAM-Chem chemistry-  
8 climate model (Community Atmospheric Model with Chemistry, version 4.0) , included into  
9 the CESM framework (Community Earth System Model, version 1.1.1) (Lamarque et al.,  
10 2012). A summary of the model setup and simulations used in this study are provided below,  
11 whereas a detailed description of the iodine chemical scheme and reaction rates is described  
12 elsewhere (Ordoñez et al., 2012; Saiz-Lopez et al. 2014).

### 13 **2.1 Model setup**

14 The model setup used for all simulations considered a horizontal grid resolution of  $1.9^\circ$   
15 (latitude)  $\times$   $2.5^\circ$  (longitude) and 26 hybrid vertical levels from the surface to approximately 40  
16 km (Lamarque et al., 2012). In order to allow the stabilization of the tropospheric conditions  
17 and to perform a direct chemical comparison between simulations representative of different  
18 time periods, all simulation schemes considered identical prescribed SST and sea-ice  
19 boundary conditions representative of year 2000 (Rayner et al., 2003). Since model results are  
20 not representative of the meteorology of any specific year, annual averages are presented. In  
21 all cases, ocean and land masks were applied to the model streaming in order to compute the  
22 global absolute and relative averages presented here.

### 23 **2.2 Ocean iodine emissions**

24 The global emission inventory of CAM-Chem was updated by the inclusion of a state-of-the-  
25 art iodine and bromine photochemical mechanism, including natural oceanic sources of VSL  
26 bromo- and iodo- carbons which have previously been validated (Ordoñez et al., 2012; Saiz-  
27 Lopez et al., 2012b). Particularly, the current work focuses on the emission of ISG emitted  
28 from the ocean after the oxidation of aqueous iodide by  $O_3$  deposited in the ocean (Garland et  
29 al., 1980) and the resulting emission of HOI and  $I_2$ . This emission function was included in  
30 CAM-Chem following the parameterisation derived by Carpenter et al. (2013):

$$1 \quad ISG = Flux(HOI) + 2 \times Flux(I_2), \quad (1)$$

2 where

$$3 \quad Flux(HOI) = [O_3] \times \left( 4.15 \times 10^5 \times \left( \frac{\sqrt{[I_{aq}^-]}}{w} \right) - \left( \frac{20.6}{w} \right) - 23600 \times \sqrt{[I_{aq}^-]} \right) \quad (2)$$

$$4 \quad Flux(I_2) = [O_3] \times [I_{aq}^-]^{1.3} \times (1.74 \times 10^9 - (6.54 \times 10^8 \times \ln w)), \quad (3)$$

5 being  $w$  the wind speed ( $m s^{-1}$ ),  $[O_3]$  the surface ozone mixing ratio ( $nmol mol^{-1}$ ) and  $[I_{aq}^-]$  the  
 6 concentration of aqueous iodide ( $mol dm^{-3}$ ) (Carpenter et al., 2013). Based on the work of  
 7 MacDonald et al. (2014), the sea surface temperature (SST, K) was used as a proxy for  
 8 describing  $[I_{aq}^-]$ :

$$9 \quad [I_{aq}^-] = 1.46 \times 10^6 \times \exp\left(\frac{-9134}{SST}\right). \quad (4)$$

10 Recently, the coincident study of Chance et al. (2014) has compiled the sparse measurements  
 11 of sea surface iodide and has also concluded SST as the best proxy to reproduce the  
 12 geographical distribution of  $[I_{aq}^-]$ . In that work the authors estimated a slightly higher  
 13 correlation coefficient between measured  $[I_{aq}^-]$  and  $SST^2$  as compared to the  $\ln[I_{aq}^-]$  and  $SST^{-1}$   
 14 correlation considered by MacDonald et al. (2014) (Eq. (4)). Nevertheless both studies  
 15 concluded on the need of further investigations for a better understanding of processes linked  
 16 to  $[I_{aq}^-]$ , its global distribution and parameterisation by means of commonly available marine  
 17 environment parameters such as SST. The iodide concentrations modelled herein after Eq.  
 18 (4), with mean values of  $50 nmol dm^{-3}$ , were in good agreement with the interquartile range of  
 19  $28-140 nmol dm^{-3}$  of the measurements compiled by Chance et al. (2014). As shown in Fig. 1,  
 20 the modelled latitudinal distribution of  $[I_{aq}^-]$  also reproduced the increasing iodide gradient  
 21 towards equatorial waters reported by Chance et al. (2014).

22 Following Eq. (1-3), CAM-Chem computed the ISG flux from the ocean considering the  
 23 modelled SST (i.e.,  $[I_{aq}^-]$ ), wind speed and surface ozone concentration for each grid-box and  
 24 time-step, resulting on an average iodine emission of  $1.9 Tg y^{-1}$  from inorganic precursors  
 25 (95% from HOI), as compared to  $0.4 Tg (I) y^{-1}$  yielding from organic sources. The modelled  
 26 geographical distribution of the ISG fluxes is shown in Fig. 2. Note that, for a given SST, the  
 27  $[I_{aq}^-]$  parameterisation after Eq. (4) results on lower iodide concentrations than considering the  
 28 abovementioned  $[I_{aq}^-]$ - $SST^2$  correlation (Chance et al., 2014). Also note that the deposition of

1 ozone to the oceans is connected to the ocean biogeochemistry (Ganzeveld et al., 2009). Thus,  
2 for instance, if the model considers the electronic affinity between iodide and ozone involved  
3 in the deposition process, the consequent emission of iodine to the atmosphere is enhanced  
4 particularly in those regions with elevated ozone pollution and high iodide concentrations.  
5 Hence the ISG fluxes modelled in this study should be regarded as lower limits.

### 6 **2.3 Present-day and pre-industrial simulations**

7 In order to assess the anthropogenic effect on the natural cycle of iodine in the MBL, two  
8 different runs were defined time-wise: present day (*PD run*) and pre-industrial time (*PI run*);  
9 representative of the emissions and resulting atmospheric chemical conditions of 2000 and  
10 1850, respectively (Lamarque et al., 2010; Myhre et al., 2013). To avoid dynamical  
11 perturbations and to compare the chemical impacts of different states of the atmosphere, all  
12 PD and PI simulations were performed in specified dynamics mode with the same high  
13 frequency meteorological input from a previous CAM-Chem 15-years simulation for year  
14 2000. Then, the horizontal wind components, air temperature, SST, sensible flux, latent heat  
15 flux and wind stress were read from a unique input meteorological dataset every 3-6 hrs  
16 (Lamarque et al., 2010). The chemical solver was initialized with boundary conditions  
17 representative of each of the periods modelled. In particular, O<sub>3</sub> initial conditions were taken  
18 from previous climatic model simulations with standard tropospheric halogen chemistry, and  
19 2 yrs of simulations were performed in order to stabilise tropospheric iodine and ozone levels.  
20 Prescribed surface concentrations of long-lived halocarbons (CFCs, halons, CH<sub>3</sub>Br and  
21 CH<sub>3</sub>Cl) were also included (Lamarque et al., 2010). Even when all simulations had the same  
22 meteorology, the model was allowed to proceed with an independent inter-annual chemical  
23 evolution of all tropospheric constituents, and a direct comparison of the oxidative capacity of  
24 different types of atmospheres (PD vs. PI) could be addressed (Lamarque et al., 2012). Note  
25 that the organic iodine emissions were considered to remain unaltered in time. Thus, the  
26 selection of a setup with equivalent meteorology for both time periods allowed us to obtain a  
27 parameterised ISG flux and resulting total inorganic iodine burden ( $I_y = I + IO + HOI + IONO_2$   
28  $+ HI + OIO + INO + INO_2 + 2 \cdot I_2 + IBr + ICl + 2 \cdot I_2O_x$  with  $x = 2-4$ ) in the marine environment  
29 dependent only on the changes in surface ozone between present and past times. Throughout  
30 this study the percentage or relative changes reported were estimated as  $100 \times (PD-PI)/PD$ .

31

### 1 **3 Results and discussion**

2 Once the current ISG flux and its global pattern have been determined (Sect. 2.2), in the  
3 following we proceed to investigate their evolution since 1850 as well as the implications of  
4 such evolution.

#### 5 **3.1 Change in ozone and atmospheric inorganic iodine since pre-industrial** 6 **times**

7 Figure 3 shows the geographical distribution of the modelled present-day ozone burden in the  
8 MBL and its change since pre-industrial times (Lamarque et al. 2010). In agreement with  
9 observations (Myhre et al., 2013), our simulations indicate that anthropogenic activities since  
10 1850 have caused a mean ozone increase of 40% in MBL. As a result of the deposition and  
11 subsequent reaction of ozone with iodide in the surface ocean, our results reveal that the  
12 human-mediated increase in ozone levels has yielded a rise of the global oceanic ISG flux  
13 from 1.04 Tg (I)  $y^{-1}$  emitted in 1850, to 1.9 Tg (I)  $y^{-1}$  emitted currently. That ISG flux rise of  
14 45% (Fig. 4) has caused a similar increase in the total inorganic iodine budget of the global  
15 MBL over the last two centuries (Fig. 5). Human activities including industrial processes,  
16 energy use and agricultural activities have had a more pronounced effect in the northern  
17 hemisphere where anthropogenic emissions of ozone precursors have dramatically increased  
18 since the industrial revolution (Volz and Kley 1988; Lamarque et al., 2010; Myhre et al.,  
19 2013) (Fig. 3b). Consequently, the anthropogenic amplification of the natural oceanic  
20 emission of iodine and, therefore the  $I_y$  abundance in the MBL, also reflects a strong north  
21 (NH) to south (SH) hemispheric gradient as shown in Fig. 5.

#### 22 **3.2 Change in iodine-mediated ozone loss rate since pre-industrial times**

23 Considering all the ozone depleting families (i.e., odd oxygen, hydrogen, nitrogen, iodine,  
24 bromine, chlorine) (Brasseur and Solomon, 2005, see also Saiz-Lopez et al., 2014), we  
25 calculate that the industrialisation process has on average increased the rate of the total ozone  
26 chemical loss in the global MBL from 1.89  $\text{nmol mol}^{-1} \text{d}^{-1}$  to 3.19  $\text{nmol mol}^{-1} \text{d}^{-1}$ , mainly  
27 driven by changes in the abundance of odd oxygen, hydrogen and iodine. On a global annual  
28 average, 25% of that enhanced ozone loss rate results from the human-driven boosting of  
29 inorganic iodine emissions that has accelerated iodine-mediated ozone destruction from 0.54  
30  $\text{nmol mol}^{-1} \text{d}^{-1}$  in pre-industrial times, to 0.89  $\text{nmol mol}^{-1} \text{d}^{-1}$  in the present-day. Figure 6

1 depicts the ozone loss rates by the different chemical families in the present-day scheme. As  
2 shown in Fig. 7, the ozone-driven increase in iodine emissions since PI times has resulted in a  
3 remarkable acceleration of ozone loss in the global MBL with a strong hemispheric gradient.  
4 We calculate that since 1850 the total surface O<sub>3</sub> loss rate has increased by 2.1 and 0.6 nmol  
5 mol<sup>-1</sup> d<sup>-1</sup> in NH and SH, respectively. When only the contribution of the iodine cycle is  
6 considered, hemispheric annual changes in the O<sub>3</sub> loss rate are 0.5 and 0.2 nmol mol<sup>-1</sup> d<sup>-1</sup> in  
7 NH and SH, respectively (Fig. 7). Notably, iodine was and still is the second strongest ozone  
8 depleting family in the MBL, being responsible for about 30% of the total ozone loss in that  
9 region of the atmosphere (Fig. 6). Integrating the tropospheric column, the rate of iodine-  
10 catalyzed ozone destruction has increased by 90 Tg y<sup>-1</sup> since the pre-industrialisation era,  
11 yielding a total present day tropospheric ozone removal by iodine of 280 Tg y<sup>-1</sup>.

12 In general, marine regions surrounding northern developed and developing countries, and  
13 areas connecting them, have undergone the strongest amplification of the natural cycle of  
14 inorganic iodine emissions as a result of the enhanced deposition of ozone to those regions of  
15 the ocean (Figs. 4-7). Remarkably, the current anthropogenic influence maximizes in highly  
16 polluted coastal regions such as the East-South China Sea, the South Bay of Bengal, the Gulf  
17 of Mexico and California's offshore waters (Fig. 3) where we calculate an increase of up to  
18 70% in atmospheric iodine since PI times (Fig. 5). In these regions of continental ozone-rich  
19 outflow the iodine-mediated ozone loss rate in recent times has accelerated by a similar factor,  
20 i.e. about 6 times more (up to 2 nmol mol<sup>-1</sup> d<sup>-1</sup>) than the global average of 0.35 nmol mol<sup>-1</sup> d<sup>-1</sup>  
21 (Figs. 6 and 7).

### 22 **3.3 Iodine-mediated change in ozone radiative forcing since pre-industrial** 23 **times**

24 Due to its long-wave absorption, present-day tropospheric ozone RF is estimated to be in the  
25 range of 0.2-0.6 W m<sup>-2</sup> (Myhre et al., 2013). Investigating the effect of the ISG flux in the  
26 budget of ozone in the tropospheric column and following the methodology of Saiz-Lopez et  
27 al. (2012b), we calculate that the tropospheric ozone depletion caused by current ocean  
28 emissions of inorganic iodine reduces the warming effect of ozone in the global marine  
29 troposphere by 3-10%, up to 20% on average in the NH. Note however that these values  
30 should be regarded as lower limits. Based on the recent study of Saiz-Lopez et al. (2014), we  
31 investigated the effect that the photolysis of the higher oxides I<sub>2</sub>O<sub>x</sub> (x = 2, 3, or 4) formed  
32 after the reactions of IO with itself (x = 2), and with OIO (x = 3), or OIO with itself (x = 4)

1 (Bloss et al., 2001; Spietz et al., 2005; Gómez Martín et al., 2005 and 2007; Saiz-Lopez et al.,  
2 2008) could have on the RF of tropospheric ozone. Our results indicate that if the photolysis  
3 of  $I_2O_x$  is considered, the current negative effect of the enhanced iodine-mediated ozone loss  
4 in the marine troposphere would mitigate the warming long-wave radiative effect of  
5 tropospheric ozone by up to 20% globally, and up to 40% in the NH.

6 As compared to 1850, we estimate that the abovementioned 45% increase in  $I_y$  loading has  
7 yielded a significant decrease in the RF associated with tropospheric ozone, reinforcing the  
8 need of a better process-level understanding of the uncertainties in atmospheric iodine  
9 chemistry in order to assess the impact of iodine on the tropospheric ozone RF and its future  
10 trends.

### 11 **3.4 Geochemical feedback mechanism**

12 In this study we suggest that the human-driven increase of tropospheric ozone has led to an  
13 amplification of the natural cycle of iodine emissions that has consequently decreased the  
14 lifetime of ozone in the marine atmosphere, thus closing a negative feedback loop as  
15 conceptually illustrated in Fig. 8. The result of this geochemical feedback mechanism  
16 indicates that ocean emissions of iodine act as a natural buffer of anthropogenic ozone  
17 pollution and its associated RF in the marine troposphere. Despite possible model  
18 uncertainties (e.g. in the parameterisation of ISG flux, dependence of ozone deposition on  
19 ocean biogeochemistry or possible changes in climatological parameters since PI times), note  
20 that the establishment of this feedback mechanism is inherent to the experimentally proven  
21 dependence of inorganic iodine emissions upon the deposition of ozone to the oceans  
22 (Garland et al., 1980; Carpenter et al., 2013; MacDonald et al., 2014).

## 23 **4 Summary and conclusions**

24 After investigating past and present interactions of iodine and ozone in the open marine  
25 environment, we conclude that the enhanced injection of iodine into the present-day  
26 atmosphere, as compared to pre-industrial times, represents a mechanism by which  
27 anthropogenic activities have increased the overall reactivity of the atmosphere and have  
28 amplified the natural cycle of iodine. The human-mediated boosting of the ISG emissions has  
29 on average increased by 25% the rate of present day ozone chemical loss in the global marine  
30 environment, with regions where this increase can be up to 70%, compared with the pre-  
31 industrial era. The subsequent negative radiative forcing induced by the enhanced iodine-



1 mediated ozone depletion currently mitigates up to 20-40% the effect of tropospheric ozone  
2 as a GHG in the northern hemisphere. The human-driven enhanced iodine emissions may also  
3 have two important side implications. First, it has likely led to a larger accumulation of the  
4 iodine fraction (iodate and iodide) on marine aerosols (Baker, 2004). Second, it may have  
5 increased the input of iodine, as an essential dietary element for mammals (Whitehead, 1984)  
6 that is transported from its oceanic source to the continents.

7 The negative feedback mechanism described in this work represents a natural buffer of ozone-  
8 related pollution and its radiative forcing in the marine environment. This feedback represents  
9 a potentially important new link between climate change and tropospheric ozone since the  
10 oceanic emissions of iodine are not only linked to surface ozone, but also to SST and wind  
11 speed (both parameters with a high uncertainty regarding future trends, Rhein et al., 2013),  
12 and might also be linked to climatically driven changes in the state of the World's oceans  
13 (e.g., upwelling, acidity). All of this highlights the importance of a better understanding of  
14 background natural oceanic biogeochemical processes in currently changing environments.

15

## 16 **Acknowledgements**

17 This work was supported by the Spanish National Research Council (CSIC). The National  
18 Center for Atmospheric Research (NCAR) is funded by the National Science Foundation  
19 NSF. The Climate Simulation Laboratory at NCAR's Computational and Information Systems  
20 Laboratory (CISL) provided the computing resources (ark:/85065/d7wd3xhc). As part of the  
21 CESM project, CAM-Chem is supported by the NSF and the Office of Science (BER) of the  
22 U.S. Department of Energy. This work was also sponsored by the NASA Atmospheric  
23 Composition Modeling and Analysis Program Activities (ACMAP, number NNX11AH90G).  
24 R.P.F would like to thank ANPCyT (PICT-PRH 2009-0063) for financial support. The data  
25 supporting this article can be requested from the corresponding author A.S-L (a.saiz@csic.es).

26

## 27 **References**

- 28 Aliche, B., Hebestreit, K., Stutz, J., and Platt, U.: Iodine oxide in the marine boundary layer,  
29 *Nature*, 397, 572-573, 1999.
- 30 Baker, A. R.: Inorganic iodine speciation in tropical Atlantic aerosol, *Geophys. Res. Lett.*, 31,  
31 L23S02, doi:10.1029/2004GL020144, 2004.

- 1 Bloss, W. J., Rowley, D. M., Cox, R. A., and Jones, R. L.: Kinetics and Products of the IO  
2 Self-Reaction, *J. Phys. Chem. A*, 105, 7840-7854, 10.1021/jp0044936, 2001.
- 3 Brasseur, G. P., and Solomon, S.: *Aeronomy of the Middle Atmosphere: Chemistry and*  
4 *Physics of the Stratosphere and Mesosphere*, Springer, 2005.
- 5 Carpenter, L. J., Archer, S. D., and Beale, R.: Ocean-atmosphere trace gas exchange, *Chem.*  
6 *Soc. Rev.*, 41, 6473-6506, 10.1039/C2CS35121H, 2012.
- 7 Carpenter, L. J., MacDonald, S. M., Shaw, M. D., Kumar, R., Saunders, R. W., Parthipan, R.,  
8 Wilson, J., and Plane, J. M. C.: Atmospheric iodine levels influenced by sea surface emissions  
9 of inorganic iodine, *Nature Geosci*, 6, 108-111, 2013.
- 10 Chance, R., Baker, A. R., Carpenter, L., and Jickells, T. D.: The distribution of iodide at the  
11 sea surface, *Environmental Science: Processes & Impacts*, 16, 1841-1859,  
12 10.1039/C4EM00139G, 2014.
- 13 Ganzeveld, L., Helmig, D., Fairall, C. W., Hare, J., and Pozzer, A.: Atmosphere-ocean ozone  
14 exchange: A global modeling study of biogeochemical, atmospheric, and waterside turbulence  
15 dependencies, *Global Biogeochem. Cycles*, 23, GB4021, 10.1029/2008GB003301, 2009.
- 16 Garland, J. A., Elzerman, A. W., and Penkett, S. A.: The Mechanism for Dry Deposition of  
17 Ozone to Seawater Surfaces, *J. Geophys. Res.*, 85, 7488-7492, 1980.
- 18 Gómez Martín, J. C., Spietz, P., and Burrows, J. P.: Spectroscopic studies of the I<sub>2</sub>/O<sub>3</sub>  
19 photochemistry: Part 1: Determination of the absolute absorption cross sections of iodine  
20 oxides of atmospheric relevance, *J. Photochem. Photobiol., A*, 176, 15-38, 2005.
- 21 Gómez Martín, J. C., Spietz, P., and Burrows, J. P.: Kinetic and Mechanistic Studies of the  
22 I<sub>2</sub>/O<sub>3</sub> Photochemistry, *J. Phys. Chem. A*, 111, 306-320, 2007.
- 23 Gómez Martín, J. C., Mahajan, A. S., Hay, T. D., Prados-Román, C., Ordóñez, C.,  
24 MacDonald, S. M., Plane, J. M. C., Sorribas, M., Gil, M., Paredes Mora, J. F., Agama Reyes,  
25 M. V., Oram, D. E., Leedham, E., and Saiz-Lopez, A.: Iodine chemistry in the eastern Pacific  
26 marine boundary layer, *Journal of Geophysical Research: Atmospheres*, 118, 887-904,  
27 10.1002/jgrd.50132, 2013.
- 28 Großmann, K., Frieß, U., Peters, E., Wittrock, F., Lampel, J., Yilmaz, S., Tschritter, J.,  
29 Sommariva, R., von Glasow, R., Quack, B., Krüger, K., Pfeilsticker, K., and Platt, U.: Iodine

1 monoxide in the Western Pacific marine boundary layer, *Atmos. Chem. Phys.*, 13, 3363-3378,  
2 10.5194/acp-13-3363-2013, 2013.

3 Jones, A. E., Anderson, P. S., Wolff, E. W., Roscoe, H. K., Marshall, G. J., Richter, A.,  
4 Brough, N., and Colwell, S. R.: Vertical structure of Antarctic tropospheric ozone depletion  
5 events: characteristics and broader implications, *Atmos. Chem. Phys.*, 10, 7775-7794,  
6 10.5194/acp-10-7775-2010, 2010.

7 Lamarque, J. F., Bond, T. C., Eyring, V., Granier, C., Heil, A., Klimont, Z., Lee, D., Liousse,  
8 C., Mieville, A., Owen, B., Schultz, M. G., Shindell, D., Smith, S. J., Stehfest, E., Van  
9 Aardenne, J., Cooper, O. R., Kainuma, M., Mahowald, N., McConnell, J. R., Naik, V., Riahi,  
10 K., and van Vuuren, D. P.: Historical (1850–2000) gridded anthropogenic and biomass  
11 burning emissions of reactive gases and aerosols: methodology and application, *Atmos.*  
12 *Chem. Phys.*, 10, 7017-7039, 10.5194/acp-10-7017-2010, 2010.

13 Lamarque, J. F., Emmons, L. K., Hess, P. G., Kinnison, D. E., Tilmes, S., Vitt, F., Heald, C.  
14 L., Holland, E. A., Lauritzen, P. H., Neu, J., Orlando, J. J., Rasch, P. J., and Tyndall, G. K.:  
15 CAM-chem: description and evaluation of interactive atmospheric chemistry in the  
16 Community Earth System Model, *Geosci. Model Dev.*, 5, 369-411, 10.5194/gmd-5-369-2012,  
17 2012.

18 Lawler, M. J., Mahajan, A. S., Saiz-Lopez, A., and Saltzman, E. S.: Observations of I<sub>2</sub> at a  
19 remote marine site, *Atmos. Chem. Phys.*, 14, 2669-2678, 10.5194/acp-14-2669-2014, 2014.

20 MacDonald, S. M., Gómez Martín, J. C., Chance, R., Warriner, S., Saiz-Lopez, A., Carpenter,  
21 L. J., and Plane, J. M. C.: A laboratory characterisation of inorganic iodine emissions from the  
22 sea surface: dependence on oceanic variables and parameterisation for global modelling,  
23 *Atmos. Chem. Phys.*, 14, 5841-5852, 10.5194/acp-14-5841-2014, 2014.

24 Mahajan, A. S., Plane, J. M. C., Oetjen, H., Mendes, L., Saunders, R. W., Saiz-Lopez, A.,  
25 Jones, C. E., Carpenter, L. J., and McFiggans, G. B.: Measurement and modelling of  
26 tropospheric reactive halogen species over the tropical Atlantic Ocean, *Atmos. Chem. Phys.*,  
27 10, 4611-4624, 10.5194/acp-10-4611-2010, 2010.

28 Mahajan, A. S., Gómez Martín, J. C., Hay, T. D., Royer, S. J., Yvon-Lewis, S., Liu, Y., Hu,  
29 L., Prados-Roman, C., Ordóñez, C., Plane, J. M. C., and Saiz-Lopez, A.: Latitudinal  
30 distribution of reactive iodine in the Eastern Pacific and its link to open ocean sources,  
31 *Atmos. Chem. Phys.*, 12, 11609-11617, 10.5194/acp-12-11609-2012, 2012.

1 Myhre, G., D. Shindell, D., Bréon, F.-M., Collins, W., Fuglestvedt, J., Huang, J., Koch, D.,  
2 Lamarque, J.-F., Lee, D., Mendoza, B., Nakajima, T., Robock, A., Stephens, G., Takemura, T.  
3 and Zhang, H.: Anthropogenic and Natural Radiative Forcing. In: *Climate Change 2013: The*  
4 *Physical Science Basis. Contribution of Working Group I to the Fifth Assessment Report of*  
5 *the Intergovernmental Panel on Climate Change* [Stocker, T.F., D. Qin, G.-K. Plattner, M.  
6 Tignor, S.K. Allen, J. Boschung, A. Nauels, Y. Xia, V. Bex and P.M. Midgley (eds.)].  
7 Cambridge University Press, Cambridge, United Kingdom and New York, NY, USA, Chap.  
8 8, 2013.

9 Ordóñez, C., Lamarque, J. F., Tilmes, S., Kinnison, D. E., Atlas, E. L., Blake, D. R., Sousa  
10 Santos, G., Brasseur, G., and Saiz-Lopez, A.: Bromine and iodine chemistry in a global  
11 chemistry-climate model: description and evaluation of very short-lived oceanic sources,  
12 *Atmos. Chem. Phys.*, 12, 1423-1447, 10.5194/acp-12-1423-2012, 2012.

13 Rayner, N. A., Parker, D. E., Horton, E. B., Folland, C. K., Alexander, L. V., Rowell, D. P.,  
14 Kent, E. C., and Kaplan, A.: Global analyses of sea surface temperature, sea ice, and night  
15 marine air temperature since the late nineteenth century, *Journal of Geophysical Research:*  
16 *Atmospheres*, 108, 4407, 10.1029/2002JD002670, 2003.

17 Read, K. A., Mahajan, A. S., Carpenter, L. J., Evans, M. J., Faria, B. V. E., Heard, D. E.,  
18 Hopkins, J. R., Lee, J. D., Moller, S. J., Lewis, A. C., Mendes, L., McQuaid, J. B., Oetjen, H.,  
19 Saiz-Lopez, A., Pilling, M. J., and Plane, J. M. C.: Extensive halogen-mediated ozone  
20 destruction over the tropical Atlantic Ocean, *Nature*, 453, 1232-1235, 2008.

21 Rhein, M., Rintoul, S.R., Aoki, S., Campos, E., Chambers, D., Feely, R.A., Gulev, S.,  
22 Johnson, G.C., Josey, S.A., Kostianoy, A., Mauritzen, C., Roemmich, D., Talley, L.D., and  
23 Wang, F.: Observations: Ocean. In: *Climate Change 2013: The Physical Science Basis.*  
24 *Contribution of Working Group I to the Fifth Assessment Report of the Intergovernmental*  
25 *Panel on Climate Change* [Stocker, T.F., D. Qin, G.-K. Plattner, M. Tignor, S.K. Allen, J.  
26 Boschung, A. Nauels, Y. Xia, V. Bex and P.M. Midgley (eds.)]. Cambridge University Press,  
27 Cambridge, United Kingdom and New York, NY, USA. Chap. 3, 2013.

28 Saiz-Lopez, A., Plane, J. M. C., Mahajan, A. S., Anderson, P. S., Bauguitte, S. J.-B., Jones, A.  
29 E., Roscoe, H. K., Salmon, R. A., Bloss, W. J., Lee, J. D., and Heard, D. E.: On the vertical  
30 distribution of boundary layer halogens over coastal Antarctica: implications for O<sub>3</sub>, HO<sub>x</sub>,  
31 NO<sub>x</sub> and the Hg lifetime, *Atmos. Chem. Phys.*, 8, 887-900, 2008.

1 Saiz-Lopez, A., Plane, J. M. C., Baker, A. R., Carpenter, L. J., Von Glasow, R., Gómez  
2 Martín, J. C., McFiggans, G., and Saunders, R. W.: Atmospheric Chemistry of Iodine, Chem.  
3 Rev. (Washington, DC, U. S.), 112, 1773-1804, 10.1021/cr200029u, 2012a.

4 Saiz-Lopez, A., Lamarque, J. F., Kinnison, D. E., Tilmes, S., Ordóñez, C., Orlando, J. J.,  
5 Conley, A. J., Plane, J. M. C., Mahajan, A. S., Sousa Santos, G., Atlas, E. L., Blake, D. R.,  
6 Sander, S. P., Schauffler, S., Thompson, A. M., and Brasseur, G.: Estimating the climate  
7 significance of halogen-driven ozone loss in the tropical marine troposphere, Atmos. Chem.  
8 Phys., 12, 3939-3949, 10.5194/acp-12-3939-2012, 2012b.

9 Saiz-Lopez, A., Fernandez, R. P., Ordóñez, C., Kinnison, D. E., Gómez Martín, J. C.,  
10 Lamarque, J. F., and Tilmes, S.: Iodine chemistry in the troposphere and its effect on ozone,  
11 Atmos. Chem. Phys., 14, 13119-13143, doi:10.5194/acp-14-13119-2014, 2014.

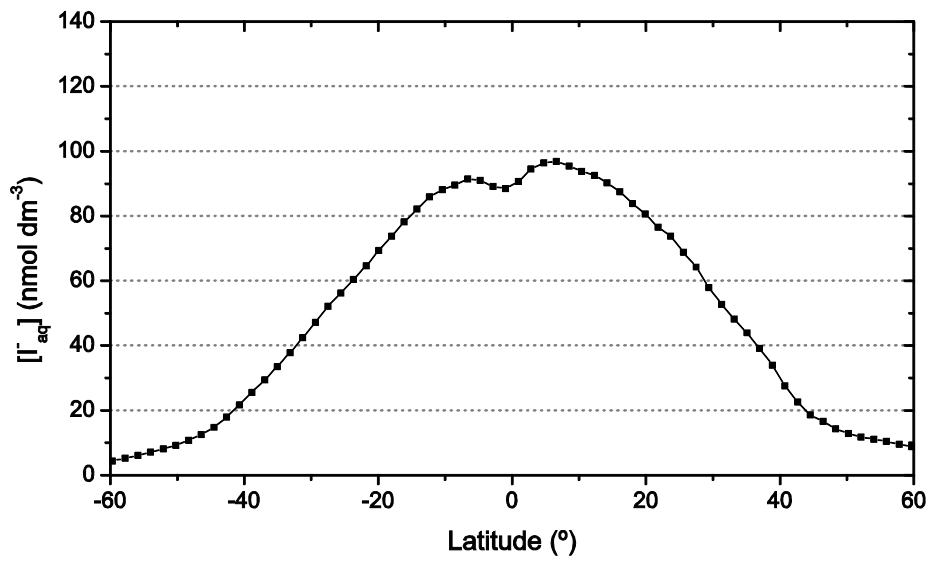
12 Spietz, P., Gómez Martín, J. C., and Burrows, J. P.: Spectroscopic studies of the I<sub>2</sub>/O<sub>3</sub>  
13 photochemistry: Part 2. Improved spectra of iodine oxides and analysis of the IO absorption  
14 spectrum, J. Photochem. Photobiol., A, 176, 50-67, 2005.

15 Volz, A., and Kley, D.: Evaluation of the Montsouris series of ozone measurements made in  
16 the nineteenth century, Nature, 332, 240-242, 1988.

17 Whitehead, D. C.: The distribution and transformations of iodine in the environment, Environ.  
18 Intern., 10, 321-339, [http://dx.doi.org/10.1016/0160-4120\(84\)90139-9](http://dx.doi.org/10.1016/0160-4120(84)90139-9), 1984.

19

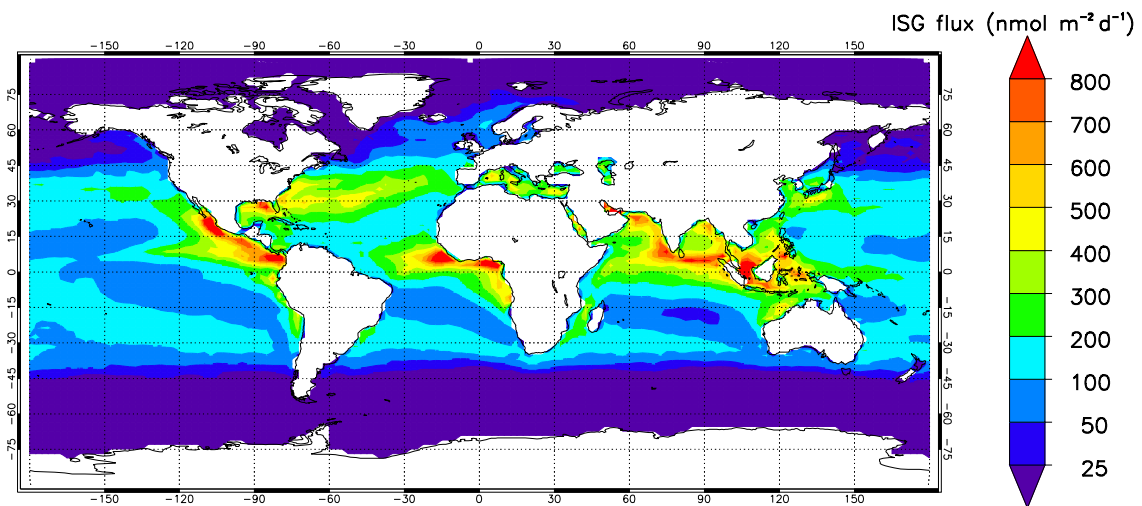
1



2

3 Figure 1. Modelled latitudinal variation of the zonal average sea surface iodide concentration,  
4 [I<sub>aq</sub>]. Following Eq. (4), [I<sub>aq</sub>] is modelled with CAM-Chem using SST as a proxy. Modelled  
5 iodide values fall within the range of [I<sub>aq</sub>] open ocean measurements reported by Chance et  
6 al. (2014), reproducing as well the iodide gradient observed towards the equator (see also  
7 Ganzelved et al., 2009).

8



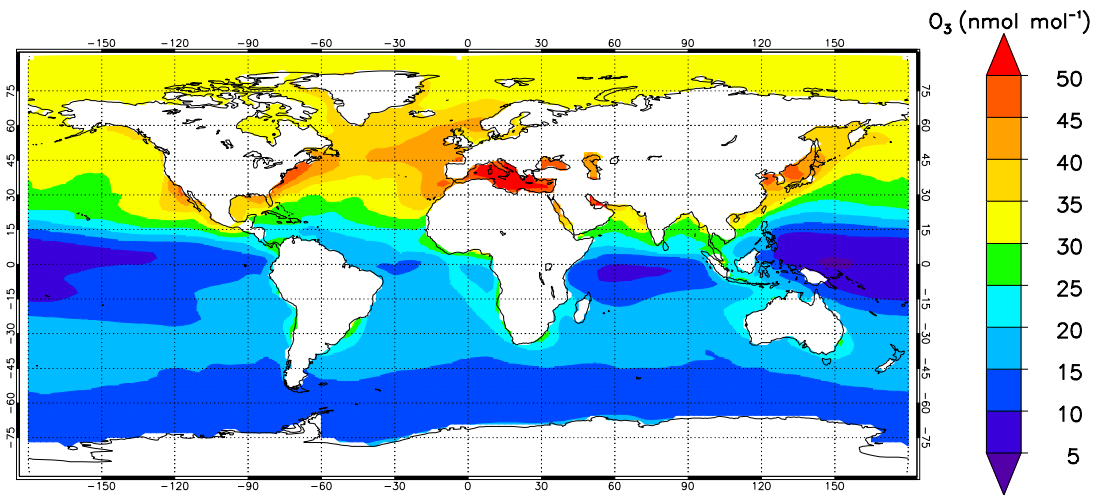
1

2 Figure 2. Modelled annual mean ocean flux of ISG. Following the laboratory work of  
3 Carpenter et al. (2013) and MacDonald et al. (2014), the parameterisation of the ISG flux  
4 given by Eq. (1-4) was newly implemented in the global chemistry-climate model CAM-  
5 Chem.

6

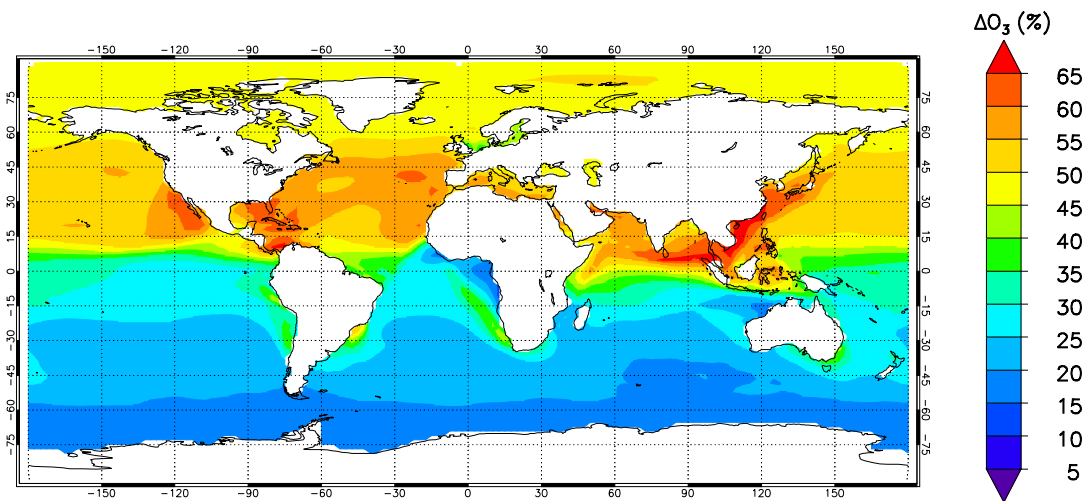
1

a



2

b

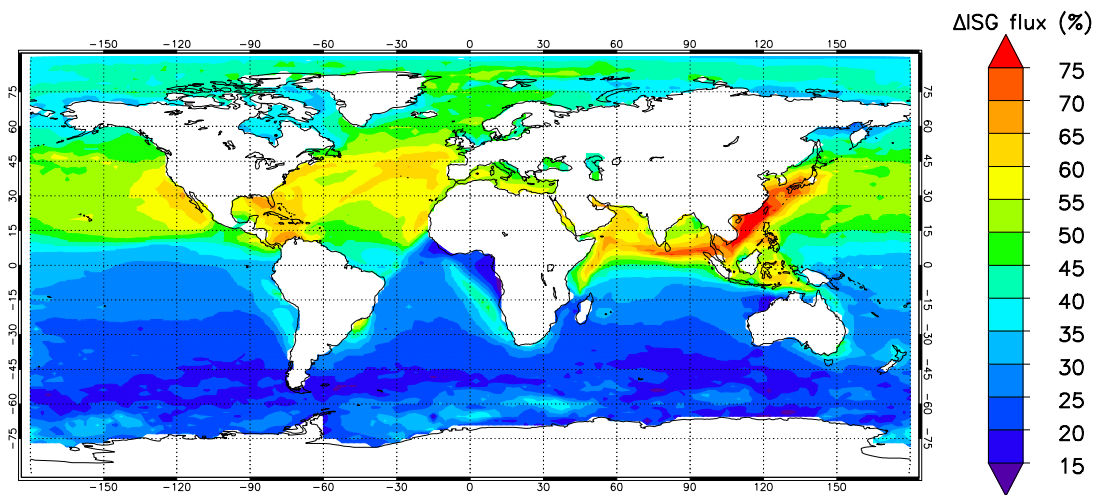


3

4 Figure 3. Modelled surface ozone in the marine environment. a. Present-day surface  $O_3$   
5 mixing ratio. b. Relative change of surface  $O_3$  mixing ratio since pre-industrial times. As a  
6 result of the hemispheric gradient on the emissions of ozone precursors (Myhre et al., 2013),  
7 the increased ozone load in the NH has doubled that of the southern hemisphere.

8

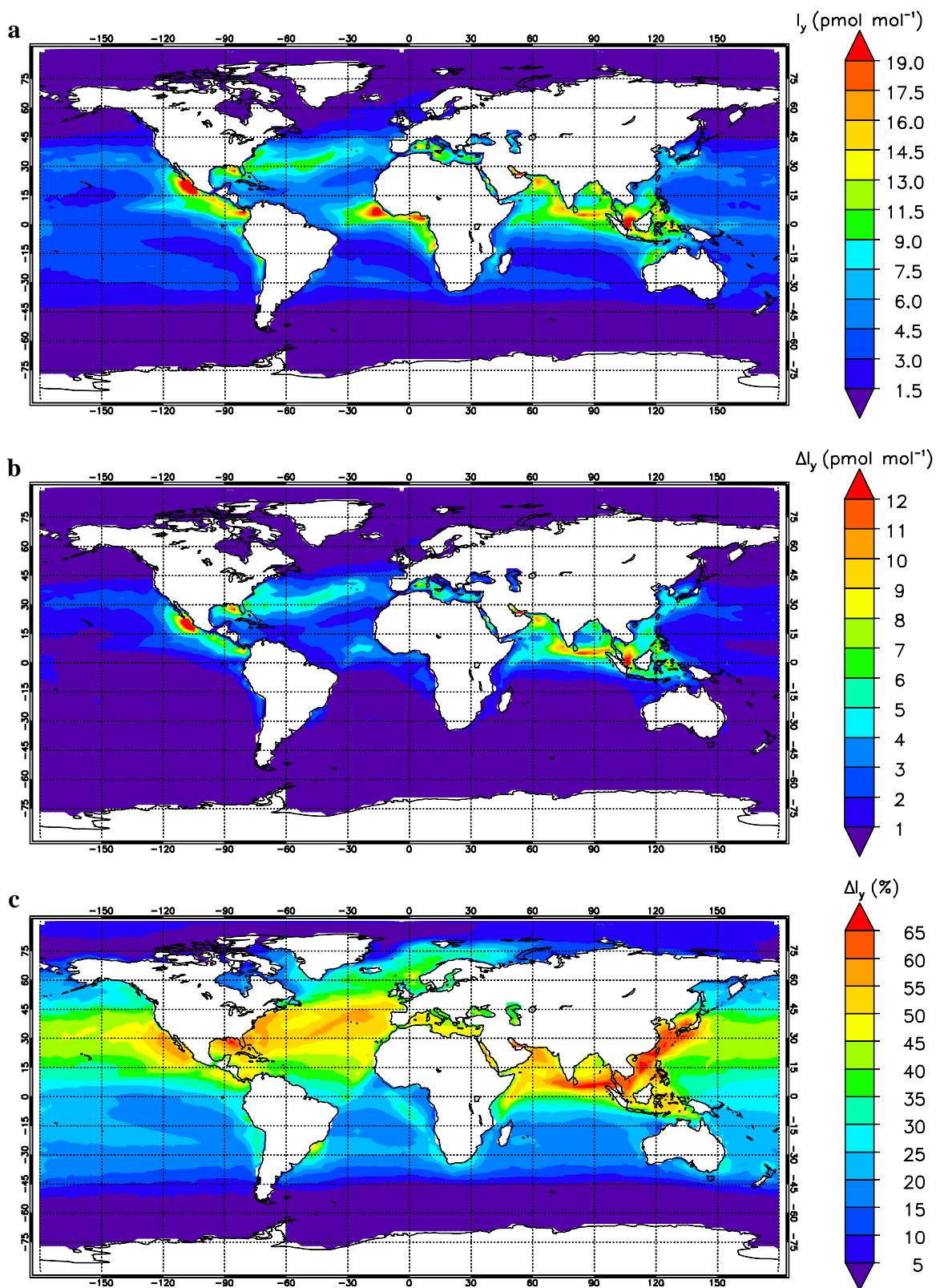




1

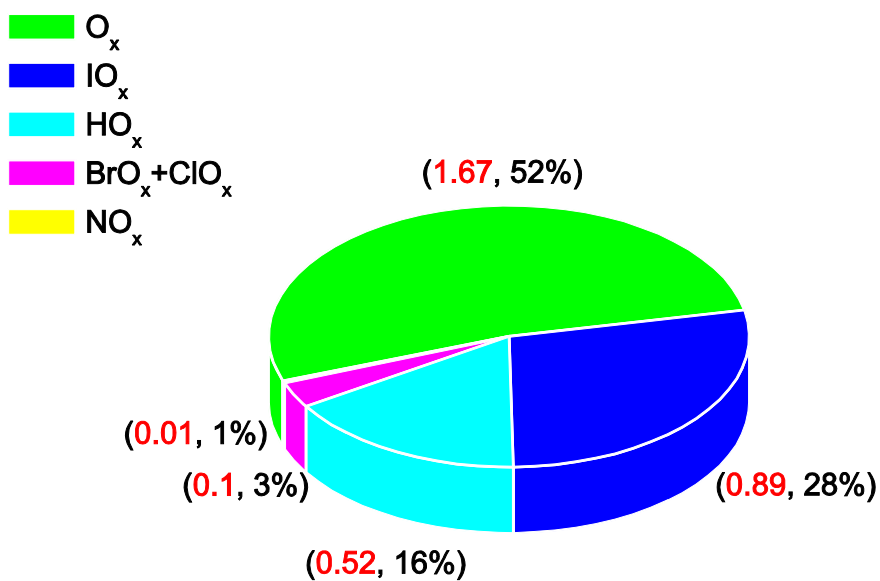
2 Figure 4. Anthropogenic influence upon the oceanic emission of inorganic iodine. The figure  
 3 presents the percentage change of the ISG fluxes since pre-industrial times. The annual  
 4 oceanic flux of ISG for the PD run is shown in Fig. 2.

5

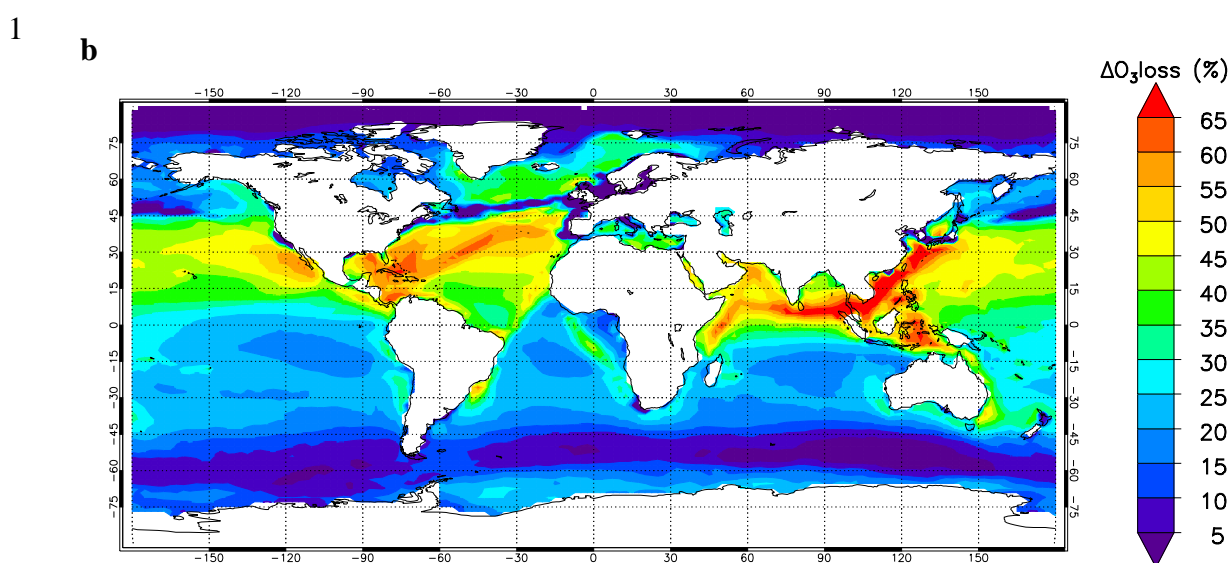
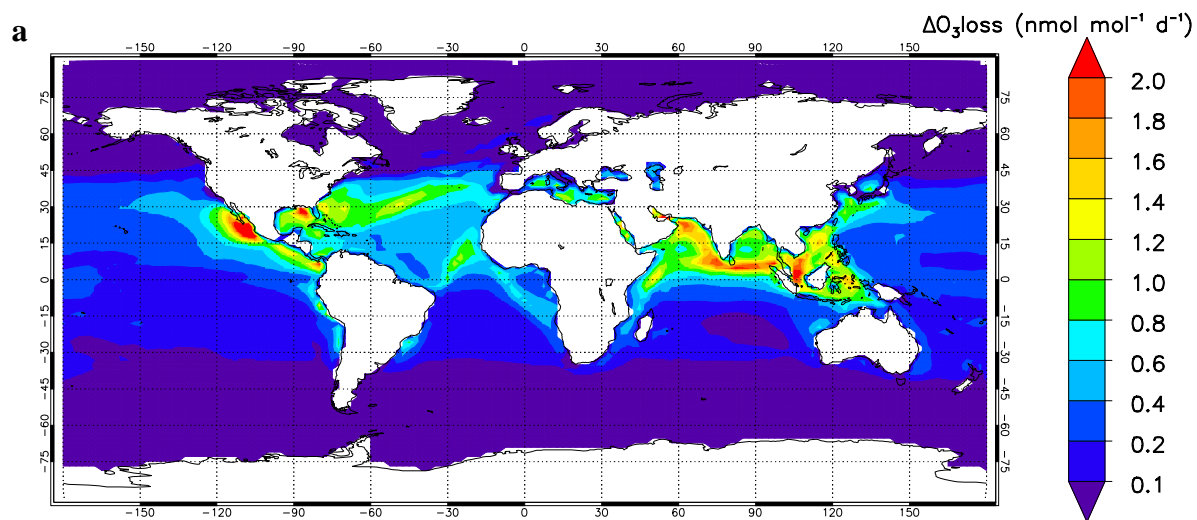


1  
 2 Figure 5. Geographical distribution of the budget of total gaseous inorganic iodine ( $I_y = I + IO$   
 3  $+ HOI + IONO_2 + HI + OIO + INO + INO_2 + 2 \cdot I_2 + IBr + ICl + 2 \cdot I_2O_x$  with  $x = 2-4$ ) in the

- 1 MBL. a. Modelled  $I_y$  mixing ratio in the PD scheme. b. Enhancement of the  $I_y$  budget since
- 2 pre-industrial times (PD-PI). c. Percentage increase of the  $I_y$  budget since industrial
- 3 revolution, i.e.,  $100 \times (\text{PD-PI})/\text{PD}$ .

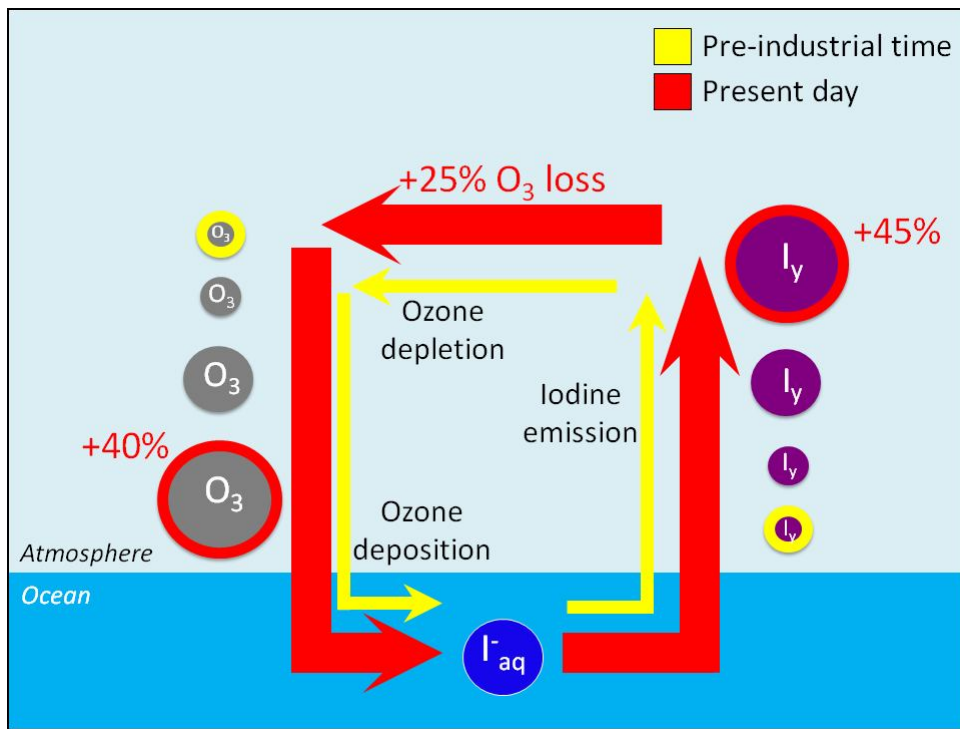


1  
 2 Figure 6. Calculated present-day ozone loss rates by the different chemical families in the  
 3 MBL (Brasseur and Solomon 2005). The first number of each parenthesis (in red) provides  
 4 the O<sub>3</sub> loss rate by the colour-coded family (in nmol mol<sup>-1</sup> d<sup>-1</sup>). The second value of each  
 5 parenthesis provides the relative contribution of each depleting family to the total ozone  
 6 chemical loss.



2  
3 Figure 7. Geographical distribution of the annual acceleration of the ozone chemical loss rate  
4 by iodine in the MBL. a. Absolute acceleration (PD-PI); b. Percentage acceleration, i.e.,  $100 \times$   
5 (PD-PI)/PD.

6



1  
 2 Figure 8. Geochemical feedback mechanism. The anthropogenic increase in tropospheric  
 3 ozone during the last two centuries (20-55%, Myhre et al., 2013) has led to an amplification  
 4 of the natural cycle of iodine emissions since pre-industrial times (PI cycle in yellow). This  
 5 has consequently decreased the lifetime of ozone in the marine atmosphere and its associated  
 6 RF, thus closing a negative feedback loop and presenting the ocean emissions of iodine as a  
 7 natural mitigating factor for anthropogenic RF in the marine environment (PD cycle in red).